

16. W. Nusselt, Ver. Deutsch. Ing. Z., 67, 206 (1923).
17. G. I. Gimbutis, in: Mechanics [in Russian], Vol. 7, Kaunas (1977), p. 92.
18. S. S. Kutateladze, Fundamentals of the Theory of Heat Transfer [in Russian], Mashgiz, Moscow-Leningrad (1962).
19. G. I. Gimbutis, Inzh.-Fiz. Zh., 23, No. 2 (1977).
20. V. I. Subbotin, P. A. Ushakov, and I. P. Sviridenko, At. Énerg., 9, No. 4 (1960).
21. E. M. Khabakhpasheva and Yu. M. Il'in, At. Énerg., 9, No. 6 (1960).
22. V. M. Borishanskii, N. I. Ivashchenko, and T. V. Zablotskaya, in: Liquid Metals [in Russian], Gosatomizdat, Moscow (1963), p. 5.
23. A. S. Andreev and D. M. Kalachev, in: Liquid Metals [in Russian], Gosatomizdat, Moscow (1963), p. 114.
24. G. I. Gimbutis and A. J. Drobavichyus, in: Mechanics [in Russian], Vol. 7, Kaunas (1977), p. 90.
25. E. G. Vorontsov and Yu. M. Tananaiko, Heat Transfer in Liquid Films [in Russian], Tekhnika, Kiev (1972).
26. R. D. Koneru, Yu. M. Tananaiko, and I. I. Chernobyl'skii, in: Chemical Machine Construction [in Russian], No. 15, Tekhnika, Kiev (1972), p. 99.
27. H. Brauer, Ver. Deutsch. Ing.-Forschungsh., 457 (1956).
28. I. I. Chernobyl'skii and E. G. Vorontsov, in: Heat and Mass Transfer [in Russian], Vol. 1, Énergiya, Moscow (1968), p. 259.

HYDRODYNAMICS OF A WATER-AIR FLOW IN A VERTICAL ANNULAR CHANNEL

É. B. Servirog and A. N. Khoze

UDC 536.24:532.529.5

Measurements on the effects of flow rate and geometrical dimensions on the hydraulic-resistance coefficient of a vertical annular channel containing a rising water-air flow are reported.

Annular channels of the tube-in-tube type are widely used in heat exchangers and the like; the heat transfer is accelerated if a gas-water mixture is used [1]. There are many papers on the hydrodynamics of such flows in pipes and channels, but similar studies for annular channels are few and rather conflicting [2, 3]. We have therefore made measurements on the hydrodynamics of water-air flows in such channels.

The working section was a vertical lucite tube having an inner diameter $d_2 = 28$ mm and length 960 mm; the internal coaxial part was a polished nonferrous tube of diameter $d_1 = 9, 12, 14, 16,$ and 24 mm or a lucite rod of diameter 20 mm. The outer tube has a length of 480 mm in the experiments with a rod of diameter 24 mm.

The centering was provided by a supporting disk and the top of the chamber. The centering device set up in the latter had interchangeable cones, which allowed us to direct the films of liquid into cyclones separately from the inner and outer surfaces of the annulus. The liquid was deposited on the walls by means of a cylindrical bubble chamber of height 70 mm and inner diameter 90 mm, which had an air-distributing grid at the bottom containing 80 holes of diameter 3 mm.

During the preliminary experiments, an equivalent diameter $d_e = 8$ mm was used to examine the effects of various designs of bubble chamber on the resistance of the working section. Although there was some variation in the distribution of the liquid over the surfaces of the annulus, the resistance was almost independent of the size and design of the bubble chamber.

The air was brought into the distributing grid by three DV-2 fans working in series. The air flow rate was measured with a Prandtl tube, an MMN-240 gauge, and a U-tube manometer, which indicated the static pressure.

Novosibirsk Electrical Engineering Institute. Translated from Inzhenerno-Fizicheskii Zhurnal, Vol. 34, No. 6, pp. 974-980, June, 1978. Original article submitted June 20, 1977.

The water circulated around a closed circuit and was passed to the bubble chamber by an ETsN-105 pump. The water flow rate was monitored and maintained by an RS-5 rotameter; the temperatures of the water and air in the bubble chamber and cyclones were monitored by mercury thermometers.

The static pressure difference Δp over the working section was monitored at eight points (or at five in the case $d_e = 4$ mm), and in each section there were three holes of diameter 0.8 mm, which were joined via an annular chamber to pressure-measuring tubes.

The liquid distribution in the annulus was recorded by fitting annular tap-off sections in the upper hollow part of the axial rod and in the outer tube, through which water was drawn off by a vacuum pump into a measuring vessel. The completeness of film collection was monitored visually from the water runoff from the cyclones and also by means of a cathode ray tube (CRT) displaying the signals from conductivity transducers.

The thickness of the films on the two surfaces were measured for $d_e = 8$ mm at 17 points by conductivity methods; a GZ-33 oscillator was used with an F-517 voltmeter and an SI-13A oscilloscope. The mean film thickness δ and the wave amplitude were determined. The speeds were as follows (m/sec): air, $w_0'' = 6-49$; water, $w_0' = (5.85-61) \cdot 10^{-3}$, which corresponded to a mean irrigation density $\Gamma_v = (1.3-9) \cdot 10^{-5}$ m²/sec.

The Reynolds number for the film Re_{d_e}' varied from 50 to 360 with these Γ_v , which corresponded to laminar flow [4].

The upper limit to the air speed was governed by the pressure-flow rate characteristics of the fans, while the lower limit was set by flow instability in the annulus.

The results for air gave ξ in good agreement with Blasius's formula: For example, the deviations did not exceed 5% for $d_e = 12$ mm or 7% for $d_e = 19$ mm.

A profile recorder indicated that the surface roughness of the outer tube did not exceed 0.012 mm, as against 0.0015-0.003 mm for the rods.

The vigorous heat and mass transfer in the bubble chamber ensured quasiisothermal conditions, and so the variations in water and air temperatures along the channel were not more than 0.2-0.7°C. All measurements were made between +15 and +22°C, the exact value being dependent on the environmental conditions.

It was found that the static pressure fell linearly along the working part of the channel.

The observations on $\Delta p/l = f(w_0'')$ gave resistance figures lower than those given by standard formulas for vertical tubes [5-8]. The discrepancy became less as w_0'' fell or d_e increased, which is in agreement with the results for steam-water flows [2].

Our measurements agree best with the measurements of [3] on the hydraulic resistance of annular channels with water injection.

We use the coefficient ξ as the dimensionless characteristic of the hydraulic resistance, which is given by Darcy's formula:

$$\Delta p = \xi \frac{l}{d_e} \cdot \frac{\rho'' w_0''^2}{2} \quad (1)$$

The measured ξ was then put in the following form [9]:

$$\xi = \xi_0 + \Delta \xi, \quad (2)$$

where ξ_0 was derived from Blasius's formula via the Reynolds number for the gas phase.

Calculations from the energy equation for $d_e = 8$ mm showed that the overall effect of the acceleration arising from the density change in the air was merely to alter the loss of heat by 2.5% (or less).

Published data [4, 9] were used in approximating the data for the increment in the hydraulic-resistance coefficient arising from liquid injection in the form

$$\Delta \xi \sim \left(\frac{w_0'}{w_0} \right)^m Re_{d_e}'^k \quad (3)$$

Figure 1 shows $\Delta\xi$ in relation to the ratio of the reduced velocities and Reynolds numbers for the liquid phase for the annuli $d_e = 8$ mm; there is a tendency for the curves to separate in accordance with the value of Re_{d_e}'' , which indicates that $k = 0$ for a certain range in w_0'' , so (3) can be simplified to

$$\Delta\xi \sim \left(\frac{w_0''}{w_0}\right)^m. \quad (4)$$

We found that the reduced gas speed corresponding to onset of separation between the straight lines varied only within the narrow limits of 26 and 20 m/sec, with a tendency to decrease as the irrigation density increased.

We used the mean irrigation density $\Gamma_V = 6.18 \times 10^{-5}$ m²/sec (Fig. 2) and also $\Gamma_V = 2.77 \cdot 10^{-5}$ m²/sec in examining the effects of the geometry of the hydraulic resistance; we found that the curves tended to separate at w_0''/w_0' below certain values, which were dependent on the channel geometry and liquid flow rate. The value of w_0'' corresponding to the onset of separation varied within narrow limits. For instance, as d_e/d_2 increased, for $Re_{d_e}' = 250$ and 110 there was a rise in that speed from 25 to 29 m/sec.

In general, the speed corresponding to onset of separation between the lines (Figs. 1 and 2) is $w_0'' \approx 25$ m/sec.

Figure 3 shows regression lines drawn up for $\Delta\xi$; at $w_0'' < 25$ m/sec,

$$\Delta\xi = 4 \cdot 10^8 Re_{d_e}'^{-1.45} \left(\frac{d_e}{d_2}\right)^{1.52} \left(\frac{w_0''}{w_0}\right)^{-2}, \quad (5)$$

and at $w_0'' > 25$ m/sec,

$$\Delta\xi = 17.2 \cdot \left(\frac{w_0''}{w_0}\right)^{-0.9}. \quad (6)$$

The appreciable increase in $\Delta\xi$ for $w_0'' < 25$ m/sec shown by (5) appears to be due to some increase in the loss involved in oversoming the gravitational force arising from a fall in the true gas content, in addition to any effects from wave formation.

The maximum deviation of the observed points from the predicted ξ is 6.2% for (6) and 19% for (5).

Figure 4 gives a general evaluation of the processes in the channel, and this shows the mean film thickness δ for each of the surfaces for $d_e = 8$ mm as a function of w_0'' for various irrigation densities.

Similar relationships apply for the wave amplitude Δ and the volume irrigation densities on the outer and inner surfaces.

The curves of Fig. 4a correspond to $\Gamma_V = 2.77 \cdot 10^{-5}$ m²/sec while those of Fig. 4b correspond to $\Gamma_V = 6.18 \cdot 10^{-5}$ m²/sec.

The film thicknesses were measured as the averages in time and over the length of the channel: δ_i for the inner surface and δ_o for the outer one.

For relatively low irrigation densities (Fig. 4a) and $w_0'' > 25$ m/sec we found that δ_o was only slightly larger than δ_i , although $\Gamma_{V_i} > \Gamma_{V_o}$; it is clear that in this case the flow conditions differ for the two surfaces. Further, δ_o increases more rapidly with Γ_V (Fig. 4b).

The mean film thickness and the wave amplitude tend to increase as w_0'' falls; reduced gas speeds of less than 25 m/sec cause particularly rapid increase in δ_o as well as in Δ_i and Δ_o . The wave amplitudes are almost identical on the two surfaces for $w_0'' > 25$ m/sec whereas Δ_o is greater than Δ_i for $w_0'' < 25$ m/sec.

The mean wave amplitudes were determined as the differences between the minimal and maximal film thicknesses at several points uniformly distributed over the height; CRT waveforms showed that w_0'' greater than $w_{T''}$ corresponding to the onset of separation (Figs. 1 and 2) resulted in almost smooth films with long waves on both surfaces, which could be seen clearly by eye on account of the very low frequency.

As the gas speed fell, waves of very much higher frequency began to appear on the long waves, and the amplitude of these increased considerably for $w_0'' < w_{T''}$, which finally resulted in the liquid films meeting and the flow becoming unstable.

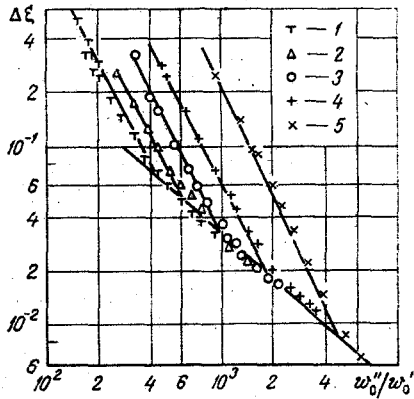


Fig. 1

Fig. 1. Measurements for channel with $d_e = 8$ mm [1) $Re'_{d_e} = 360$; 2) 248; 3) 182; 4) 108; 5) 50].

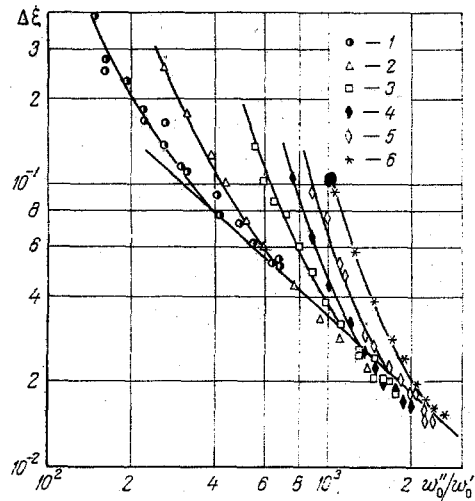


Fig. 2

Fig. 2. Effects of geometrical parameters of annular channels on $\Delta\xi$ for $Re'_{d_e} = 250$; $\Gamma_V = 6.18 \cdot 10^{-5}$ m²/sec [1) $d_1 = 24$ mm; 2) 20; 3) 16; 4) 14; 5) $d_e/12$; 6) 9 mm].

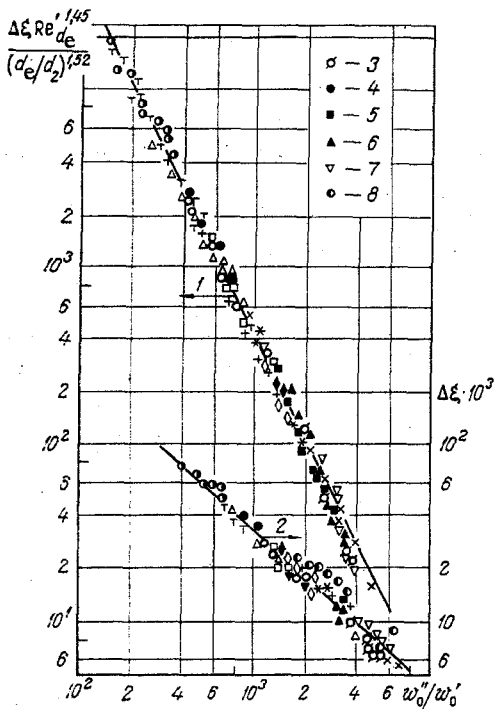


Fig. 3

Fig. 3. Regression lines for ξ [1) from (5); 2) from (6); 3) our data for $Re'_{d_e} = 109$ for $d_e/d_2 = 0.572$; 4) $Re'_{d_e} = 104$; $d_e/d_2 = 0.143$; 5) 108; 0.428; 6) 111; 0.5; 7) 105; 0.678; 8) [3]]. The other points correspond to Figs. 1 and 2.

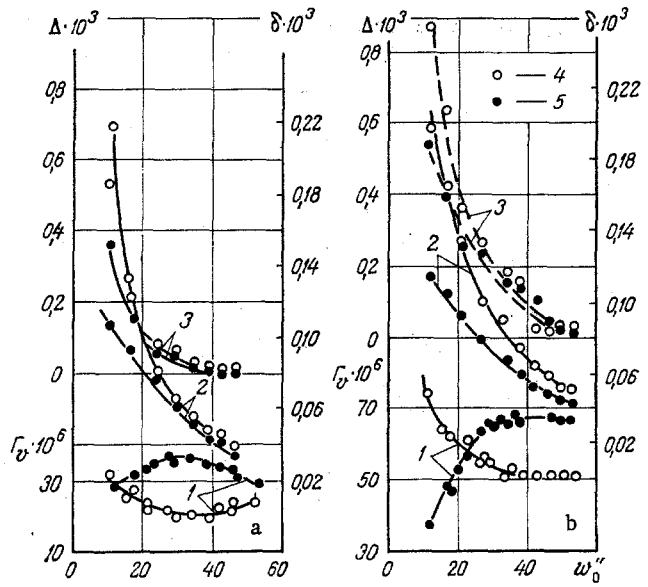


Fig. 4

Fig. 4. Distribution of liquid and film thickness over the surfaces of an annular channel with $d_e = 8$ mm for a mean volume irrigation density $\Gamma_V = 2.77 \cdot 10^{-5}$ m²/sec (a) and $\Gamma_V = 6.18 \cdot 10^{-5}$ m²/sec (b) in relation to ω_0'' , m/sec: 1) volume irrigation density; 2) mean film thickness δ , m; 3) wave amplitude Δ , m; 4) outer surface; 5) inner surface.

Increase in the outer film thickness was accompanied by redistribution of the irrigation density over the surfaces, which was particularly pronounced when w_0'' fell below the above transition speed.

The fall in irrigation density on the inner surface is due to preferential transfer of droplets from the inner surface to the outer one, although there is some fall in the general transport capacity of the gas phase.

The variations in δ and Γ_V on the surfaces for $w_0'' < w_t''$ at a given liquid flow rate are similar to those for $w_0'' > w_t''$ as the liquid flow rate is increased, so one concludes that w_t'' represents the point of onset of rapid increase in film thickness and also in wave amplitude as the gas flow rate is reduced.

The inner surface receives rather more liquid at low liquid flow speeds; however, only the outer surface is irrigated above some limiting value (at $w_0'' \approx 25$ m/sec this is $\Gamma_V = 6.8 \cdot 10^{-5}$ m²/sec), which is due to loss of droplets from the inner surface.

This transfer may be measured as the difference between the flow rate at the inlet and the amount of liquid extracted by the vacuum pumps; it varies with Γ_V and w_0'' . The proportion of this transfer increases with w_0'' between 25 and 50 m/sec at all liquid flow rates and lies in the range 3-15%.

NOTATION

l , channel length, d_1 , inner tube diameter; d_2 , diameter of outer surface; d_e , equivalent diameter; ξ_0 , hydraulic-resistance coefficient for air; ξ , hydraulic-resistance coefficient for a two-phase flow; $\Delta\xi$, hydraulic-resistance coefficient increment; w_0' , w_0'' , reduced velocities of water and air, respectively; δ , mean thickness of liquid film; Δ , wave amplitude; Γ_V , mean volume density of irrigation; ν' , kinematic viscosity of water; ρ'' , gas phase density; $Re_{de}' = 4\Gamma_V/\nu'$, Reynolds number for liquid; Δp , hydraulic resistance. Indices: i and o , inner and outer, surfaces, respectively.

LITERATURE CITED

1. A. N. Khoze, "Organized motion of two-phase flows in pipes and channels in efficient heat-transfer devices," in: Proceedings of the Fifth All-Union Conference on Heat Transfer and Hydraulic Resistance for Two-Phase Flows in Power Plants [in Russian], Leningrad (1974).
2. V. E. Klyushnev and N. V. Tarasova, *Teploénergetika*, No. 11 (1966).
3. J. A. R. Bennett and I. D. Thornton, *Trans. Inst. Chem. Eng.*, 39, 101 (1961).
4. S. S. Kutateladze and M. N. Styrikovich, *Hydraulics of Gas-Liquid Systems* [in Russian], Gosénergoizdat, Moscow-Leningrad (1976).
5. V. K. Manolov, "A study of hydraulics and heat transfer in the flow of gas-liquid mixtures in channels," Author's Abstract of Candidate's Dissertation, Leningrad Polytechnic Institute, Leningrad (1973).
6. B. I. Konobeev et al., *Teor. Osnovy Khim. Tekhnol.*, 6, No. 1 (1972).
7. M. E. Ivanov, E. S. Arustamyan, and M. K. Rustambekov, *Khim. Prom-st'*, No. 1 (1969).
8. G. B. Wallis, *One-Dimensional Two-Phase Flow*, McGraw-Hill (1969).
9. A. A. Andreevskii, V. M. Borishanskii, and G. S. Bykov, "Hydraulics of two-phase flows in tubes and channels," in: *Heat and Mass Transfer* [in Russian], Vol. 2, Part 1, Minsk (1972).